The official journal of
INTERNATIONAL FEDERATION OF PIGMENT CELL SOCIETIES · SOCIETY FOR MELANOMA RESEARCH

PIGMENT CELL & MELANOMA Research

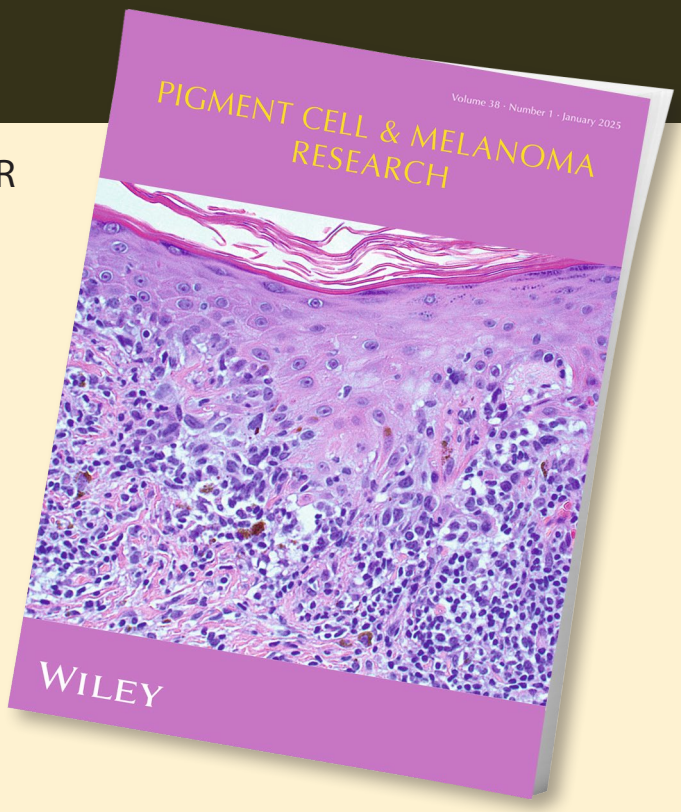

A Ball Python Colour Morph Implicates MC1R in Melanophore–Xanthophore Distribution and Pattern Formation

Alan Garcia-Elfring[1] | Heather L. Roffey[2] | Jaren M. Abergas[1] | Jurgen Wuyts[3] | Andrew P. Hendry[1] | Athanasia C. Tzika[4] | Rowan D. H. Barrett[1]

DOI: 10.1111/pcmr.13215

Volume 38, Issue 1, Pages 1-10

Pigment Cell & Melanoma Research

WILEY

ORIGINAL ARTICLE

A Ball Python Colour Morph Implicates *MC1R* in Melanophore–Xanthophore Distribution and Pattern Formation

Alan Garcia-Elfring[1] | Heather L. Roffey[2] | Jaren M. Abergas[1] | Jurgen Wuyts[3] | Andrew P. Hendry[1] | Athanasia C. Tzika[4] | Rowan D. H. Barrett[1]

[1]Department of Biology, McGill University, Montreal, Quebec, Canada | [2]Biology Department, Vanier College, Montreal, Quebec, Canada | [3]Laboratory of Molecular Cell Biology, Katholieke Universiteit Leuven, Leuven, Belgium | [4]Laboratory of Artificial & Natural Evolution (LANE), Department of Genetics & Evolution, University of Geneva, Geneva, Switzerland

Correspondence: Alan Garcia-Elfring (alan.garcia-elfring@mail.mcgill.ca) | Rowan D. H. Barrett (rowan.barrett@mcgill.ca)

Received: 27 May 2024 | **Revised:** 23 October 2024 | **Accepted:** 10 November 2024

Funding: This study was supported by NSERC Discovery Grant and Canada Research Chair to R.D.H.B. and A.P.H., a Canada Research Chair to R.D.H.B., and a Swiss National Science Foundation grant (310030_204466) to A.C.T.

Keywords: ball python | chromatophore | colour morph | genomics | *MC1R* | melanin | Mendelian phenotype | pigmentation | reptile

ABSTRACT

Reptiles showcase an extensive array of skin colours and patterns, yet little is known about the genetics of reptile colouration. Here, we investigate the genetic basis of the Clown colour morph found in captive-bred ball pythons (*Python regius*) to study skin pigmentation and patterning in snakes. We obtained samples by crowdsourcing shed skin from commercial breeders and hobbyists. We applied a case–control design, whole-genome pool sequencing, variant annotation, histological analyses, and electron microscopy imaging. We identified a missense mutation in a transmembrane region of the *melanocortin-1 receptor* (*MC1R*) associated with the Clown phenotype. In classic avian and mammalian model species, MC1R is known for controlling the type and amount of melanin produced. In contrast, our results suggest that MC1R signalling might play a key role in pattern formation in ball pythons, affecting xanthophore–melanophore distribution. This work highlights the varied functions of MC1R across different vertebrate lineages and promotes a novel model system to study reptile colouration.

1 | Introduction

The study of animal colouration has a long history in evolutionary biology (Wallace 1882; Cott 1940; reviewed by Caro 2017) and genetics (Castle and Wright 1915; Lyon 1963), because colour is an important way that species interact with their environment, and it is easily observable (Cuthill et al. 2017; Endler and Mappes 2017; Wiens and Emberts 2024). Within vertebrates, mammals and birds have one type of chromatophore, the melanocyte, which is found in the epidermis and produces the most widespread and extensively studied pigment in animals, melanin (Mills and Patterson 2009; Baxter et al. 2019). This pigment has important functions such as visual signalling, UV protection, homeostasis, host–parasite interactions and immunity (Ducrest, Keller, and Roulin 2008; Côte et al. 2018; McNamara et al. 2021). Melanin is synthesised from the amino acid tyrosine within membrane-bound organelles, called melanosomes, by the enzymes tyrosinase (TYR), Tyr-related protein 1 (TYRP1) and dopachrome tautomerase (DCT), as reviewed by Wakamatsu and Ito (2021).

In contrast, poikilothermic vertebrates, which include fish, amphibians, and non-avian reptiles, have three types of chromatophores (Bechtel 1991; Olsson, Stuart-Fox, and Ballen 2013). Like mammals and birds, reptiles produce melanin in cells called melanophores which are found in the

Summary

- Our study demonstrates that MC1R influences the distribution of xanthophores and melanophores in ball pythons, emphasising its diverse role in reptile skin colouration and broadening our understanding of pigmentation in vertebrates.

dermis and epidermis (Bechtel 1991; Megía-Palma, Jorge, and Reguera 2018). In addition, they have yellow or red cells called xanthophores or erythrophores respectively (Andrade and Carneiro 2021; Kimura 2021). These cells may contain pterins or carotenoids. Whereas pterins are synthesised endogenously from a GTP precursor, carotenoids are obtained from the diet, although they can be modified by enzymes (Toomey et al. 2022). Finally, they can also have cells with stacks of guanine crystals called iridophores that produce structural colouration. When the crystals are regularly organised, they can produce iridescence (Kuriyama et al. 2006) or act as narrowband reflectors of a specific light wavelength (Saenko et al. 2013). When disorganised, the guanine crystals act as broadband reflectors and are associated with white skin (Saenko et al. 2013).

Vertebrate colour patterning arises from cellular processes that include cell-fate specification, cell migration, and cell–cell interactions (Patterson and Parichy 2019; Subkhankulova et al. 2023). Animal colouration can vary in hue (e.g., amount of melanin; Ullate-Agote et al. 2020), pattern (e.g., solid brown vs. white spotting; Hauswirth et al. 2012) or both (Watanabe et al. 2016). Variations characterised by changes to colour (i.e., hue) but not overall patterning are often linked to genes directly involved in a pigment biosynthesis pathway (Iwanishi et al. 2018). In contrast, mutations affecting pattern (e.g., white spotting) tend to occur in genes involved in processes like cell–cell interactions through gap junction proteins (Irion et al. 2014; Usui and Watanabe 2021), differentiation or migration (Kelsh et al. 1996, 2009; Baxter et al. 2004).

Reptile species found in the pet trade provide an opportunity to advance our understanding of reptilian pigmentation. For example, captive-bred corn snakes (*Pantherophis guttatus*) have been used to uncover the lysosomal origin of chromatophore vesicles (Ullate-Agote et al. 2020) and establish gene-editing protocols in snakes (Tzika et al. 2023). The ball python (*Python regius*; Figure 1a), also known as the royal python, is another species that shows great promise (Irizarry and Bryden 2016). Over the last 30 years, ball pythons have emerged as one of the most popular snakes in the reptile trade (D'Cruze et al. 2020). Numerous Mendelian (i.e., monogenic) phenotypes affecting pigmentation and patterning ('colour morphs') have been discovered, mostly in nature, and are propagated in captivity. A few ball python morphs have been genetically characterised so far (Brown et al. 2022; Dao et al. 2023; Garcia-Elfring et al. 2023; Lederer et al. 2023), but the majority remains to be studied.

Here, we use whole-genome sequencing to study the genetic basis of a recessive ball python phenotype, the Clown colour morph (Figure 1b). Wild type ball pythons present lateral, and occasionally dorsal, patches of brown colouration on a black background. In Clown ball pythons, the lateral patches are larger and of a lighter brown colour. Although dorsal patches are not visible, regions of dark brown colouration can be observed along the dorsal midline. Thus, in this morph both the pigmentation and the pattern are affected. These differences are clearer when comparing Albino, lacking melanin, and Albino–Clown double mutants (Figure 1c,d). An additional recessive phenotype, known as the Cryptic colour morph, is considered by ball python breeders to be allelic with the Clown colour morph (Clown × Cryptic pairing results in the 'Crypton' phenotype). The Cryptic colour morph shows subtle changes in the melanin pigmentation and pattern, appearing slightly brighter and with more erratic patches relative to the wild type (Figure 1e). Clown and Cryptic both show lighter pigmentation on top of the head, referred to as a 'stamp'. We hypothesise that Clown and Cryptic share a common genetic basis, with Crypton resulting from compound heterozygosity. We identified candidate causal mutations in the *MC1R* gene associated with Clown and Cryptic that are expected to affect melanophores and their distribution in different ways.

2 | Materials and Methods

2.1 | Study Design, Sample Collection, DNA Extraction and Sequencing

We appealed to commercial breeders for ball python shed skin samples. We applied a classic case–control design, meaning we compared (pooled) DNA from case samples (i.e., samples with the Clown phenotype, $n = 38$, Table S1) against DNA from a set of control samples (i.e., samples without the Clown phenotype or mutation, $n = 21$, Table S2). The set of control samples all contain the Hypo–Ghost colour morph (Figure S1) but are known through pedigree data to not carry the Clown variant. Snakes with the Hypo–Ghost colour morph present a paler pigment phenotype (hypomelanistic) which was recently shown to be caused by a deletion in the *melanophilin* (*mlph*) gene (Lederer et al. 2023). We also compared Clown data against a control pool containing samples of the Spider colour morph (Figure S1 and Table S3). The Spider morph in ball pythons is a pattern anomaly characterised by a reduction in pattern and dark melanin pigmentation. It is also associated with pleiotropy, as Spider morph individuals frequently display abnormal head movements, a syndrome known as 'the wobble', which has been linked to malformations of the sacculus and the semicircular canals (Starck et al. 2022). In addition, we used the results from our genome-wide analysis of case–control data to test for the genetic basis of the recessive Cryptic colour morph. That is, putatively causal genes for Clown were used as candidates for Cryptic.

We extracted and sequenced DNA from shed skins by following a standard three-day phenol-chloroform procedure (Garcia-Elfring et al. 2023). Briefly, a small piece of shed skin (~2 mm × 2 mm) was digested in a lysis buffer containing proteinase K and SDS and incubated at 37°C for 24–36 h to ensure complete digestion. After digestion, we added an equal volume of phenol–chloroform–isoamyl alcohol mixture (25:24:1) and gently mixed the solution. DNA was precipitated with cold ethanol. We quantified and quality-checked DNA on an Infinite 200 Nanoquant (Tecan Group Ltd. Männedorf, Switzerland). We prepared two pools with equimolar

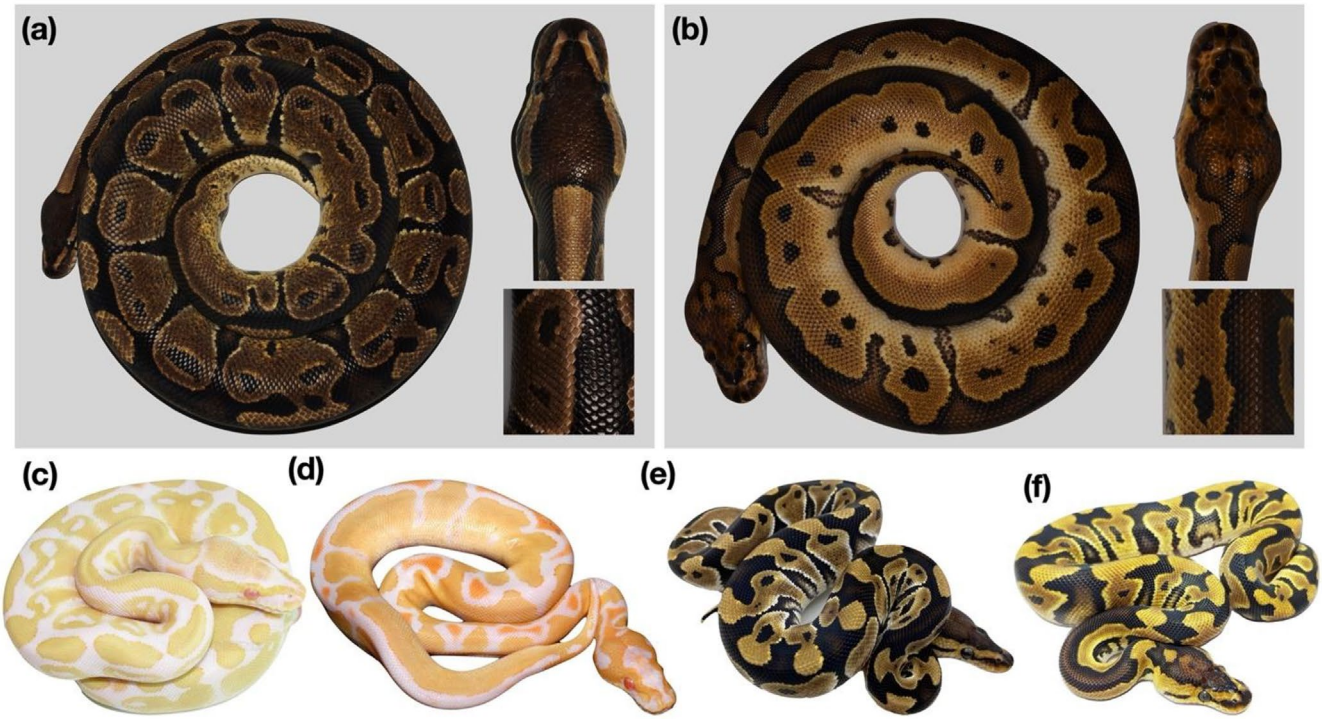

FIGURE 1 | Mendelian phenotypes in ball pythons. The wild type (a) pigmentation and pattern is contrasted with the Clown colour morph (b), which exhibits larger and brighter lateral patches, light brown coloration along the dorsal midline, and altered head pigmentation. The albino ball pythons (c) lack black pigmentation, but the pattern seems unaffected. Albino–Clown double-mutants (d) show dorsal patches of bright red coloration, possibly responsible for the light brown coloration along the dorsal midline of the Clown single mutants. The Cryptic colour morph (e) displays a subtly lighter colour and altered patches pattern relative to the wild type. Crypton animals (f) display a reduction of their black coloration relative to the wild type. Photo credits: c, d, e—worldofballpythons.com, f—Proherper.com.

amounts of each sample (10 ng/μL) (Tables S1 and S2). We sent our pooled samples to the McGill Genome Centre for whole-genome PCR-based library preparation and sequencing of 150 bp paired-end reads on one lane of the Illumina NovaSeq 6000 platform.

2.2 | Association Mapping

We first filtered raw sequence reads based on read quality (--quality-threshold 20) and length (--min-length 50) using the *trim-fastq.pl* program of *Popoolation* (Kofler et al. 2011). This process trims bases with a quality score below 20 and discards reads if the final length is < 50 bp. The Burmese python (*Python bivittatus*) is the closest relative of the ball python for which an annotated draft genome sequence is available (Castoe et al. 2013), but the *Pmo2.0* reference genome is quite fragmented, with an N50 contig size of 10.7 and 207.5 kb for the unplaced-scaffold size. Thus, to identify genomic regions of interest, we also aligned reads to the chromosome-length Burmese python reference genome *Python_molurus_bivittatus-5.0.2_HiC* (Dudchenko et al. 2017, 2018), which is not annotated. We used the annotations (GFF3) from the draft assembly (GCF_000186305.1) and mapped them to the chromosome-length assembly using the *Liftoff* program (Shumate and Salzberg 2021). To estimate sequence divergence between ball python reads and the Burmese python reference genome, we first filtered for fixed alternate alleles. Initially, we used grep to filter and count the variants in the VCF file with zero coverage for the reference allele ('DP4 = 0,0,'). Next, we used samtools depth to get the total number of sites covered during alignment. Finally, sequence divergence was estimated as the number of fixed SNPs divided by the total number of sites covered.

We aligned processed reads to both genomes using the program *bwa-mem* with default parameters (Li and Durbin 2009). We converted SAM files to BAM format with *SAMtools* (Li et al. 2009) and removed reads with mapping quality below 20 (-q 20). *SAMtools* and *Popoolation2* (Kofler, Pandey, and Schlötterer 2011) were subsequently used to produce mpileup and sync formats, respectively. We generated VCF files by using *bcftools* to call variants and filter (*vcfutils.pl varFilter*) for a minimum depth of five (-d 5) and mapping quality of 20 (-Q 20). The program *fst-sliding.pl* of *Popoolation2* was used to calculate SNP-specific F_{ST} estimates (Clown vs. Hypo–Ghost) across the genome. Because we only analysed DNA from snakes exhibiting the recessive Clown traits, the causal variant for Clown is expected to be fixed (or nearly fixed) in its respective pool and have a high F_{ST} relative to the Hypo–Ghost control pool, where the Clown allele should be missing. We generated Manhattan plots to visualise genome-wide patterns of genetic differentiation and gain insight into the location of the Clown colour morph mutation. The Clown interval was defined as the distance between the first and last SNP with an F_{ST} of 1.0 on chromosome 3. Within this region, we considered SNPs with $F_{ST} > 0.90$ rather than 1.0 to account for possible misidentification of heterozygotes for wildtype individuals in crowd-sourced samples. We conducted a Fisher's exact test

(FET) to assess significant changes in allele frequency between the Clown and reference pools (Hypo-Ghost and Spider morphs), applying the Benjamini–Hochberg method to correct for multiple hypothesis testing.

2.3 | Variant Annotation and Identification of Polymorphisms and Fixed Differences

We annotated variants with the software *SnpEff* (Cingolani et al. 2012) using the Burmese python reference genome (*Python_molurus_bivittatus-5.0.2*, assembly: GCF_000186305.1). This program predicts the effect of mutations (SNPs and small indels) on a protein. Variants within the region of interest, with an F_{ST} greater than 0.90, mapping to a gene and affecting the gene product (e.g., nonsense mutations and small indels—'high impact'; missense mutations—'moderate impact') were considered as candidate causal mutations. We used the program *Protter* (Omasits et al. 2014) to visualise *MC1R* variation relative to MC1R protein domains. We conducted a multiple sequence alignment (MSA) of MC1R using the MUSCLE algorithm (Edgar 2004) implemented in the *Jalview* software (Waterhouse et al. 2009).

We validated candidate loci by PCR amplification and Sanger sequencing *MC1R* of samples known through pedigree analysis to be heterozygotes (Table S4: Het. Clown, $n=17$; Het. Cryptic, $n=12$), homozygotes (Clown, $n=1$; Cryptic, $n=4$), and wild type (not-Clown, $n=33$; not-Cryptic, $n=35$). Primers to amplify the regions with the candidate loci were designed using *Primer3* (Kõressaar and Remm 2007; Kõressaar et al. 2018) and were the following: (Clown) Forward: 5′-ACTTCTCCAATAGCACCACTGAT-3′, Reverse: 5′-TAGAAGATGGTGATGTAGCGGTC-3′; (Cryptic) Forward: 5′-CTAGCAGCGCCACAAAGTG-3′, Reverse: 5′-CTAAGGGACCCAGCCTCTC-3′.

To increase the sample size of ball pythons genotyped at the candidate loci, we obtained 80 additional samples from breeders in Europe (Table S5). We genotyped captive-bred ball pythons from mainland Europe and the United Kingdom described by breeders as either Clown ($n=6$), heterozygous for Clown ($n=36$), non-Clown ($n=38$), Cryptic ($n=5$), heterozygous for Cryptic ($n=38$), Crypton ($n=5$), which is a double Clown–Cryptic heterozygote, and non-Cryptic ($n=37$). We hypothesise that Crypton is the result of compound heterozygosity—mutations at different loci on the same gene.

In the ball python breeding hobby, the recessive colour morphs known as Amur and Gizmo were initially treated as distinct morphs that were allelic with Cryptic and Clown. Subsequent genotyping by a private company (Proherper.com) showed that Cryptic, Amur, and Gizmo carry the same mutation as Cryptic. It remains to be seen if they carry additional mutations at this or another locus.

2.4 | Histological Analyses and Transmission Electron Microscopy Imaging

One juvenile Clown ball python was housed at the LANE animal facility under the veterinary cantonal permit no. 1008. Samples were collected following Swiss law regulations and under the experimentation permit GE24/33145. This animal was not included in the association mapping analyses described above. Skin samples from three different regions were fixed in 4% paraformaldehyde, dehydrated in ethanol, and embedded in paraffin blocks. We imaged seven-micrometer deparaffinised microtome sections with a VHX-7000 microscope (Keyence). For transmission electron microscopy, skin pieces of one mm^2 from the same three regions were processed as previously described (Ullate-Agote et al. 2020). Sample processing and imaging was performed at the Electron Microscopy Facility, University of Lausanne (Switzerland).

2.5 | Gene Nomenclature

Here, we refer to the *MC1R*/*Mc1r*/*mc1r* gene consistently as '*MC1R*' across all species, irrespective of conventional species-specific gene nomenclature. This choice was made to maintain clarity and uniformity throughout the text.

3 | Results

3.1 | Missense Mutations on the Melanocortin 1 Receptor

We compared a pool of 38 individuals of the Clown colour morph with two non-Clown pools: Hypo-Ghost ($n=21$) and Spider ($n=26$). The Clown samples have no Hypo-Ghost and no Spider variation, whereas the Hypo-Ghost and the Spider samples have no Clown variation (Tables S1–S3). Our sequencing resulted in a total of 430,722,258 reads (forward + reverse) filtered for sequence quality (minimum 20) and length (minimum 50 bp). Filtering for mapping quality and depth left a total of 227,085,378 reads mapped to the reference Burmese python genome. We found that sequence divergence between ball python reads and the reference genome is 0.0218 (2.18%). Our sequencing of the Clown pool resulted in an average coverage of 36.9 for sites with non-zero coverage (34.1 across all sites). The two reference pools, Hypo–Ghost and Spider, showed an average coverage of 26.3 (all sites: 24.3) and 32.5 (all sites: 30.1), respectively.

A genome-wide scan of allele frequency differences, as shown by F_{ST}, reveals a 3.23 Mb region of Chromosome 3 (chromosome 3:667,960–3,296,430) with fixed SNPs ($F_{ST}=1.0$) relative to Hypo–Ghost (Figure 2a). There is an additional peak on Chromosome 2 associated with the Hypo–Ghost colour morph. The region of high differentiation on Chromosome 2 contains the gene *MLPH*, which was recently linked to the Hypo–Ghost phenotype (Lederer et al. 2023). We find an overlapping interval on Chromosome 3 (3:67,960–4,702,200) when comparing the Clown pool to the Spider pool, supporting the association of this genomic region with the Clown phenotype (Figure 2b). A Fisher's exact test between Clown and both Hypo–Ghost and Spider further confirms the association in chromosome 3 (Figure S3).

We found 98 genes (748 variants, including 7 indels in non-coding regions) annotated within the region of high differentiation on Chromosome 3 from 667,960 to 3,296,430 (Table S6).

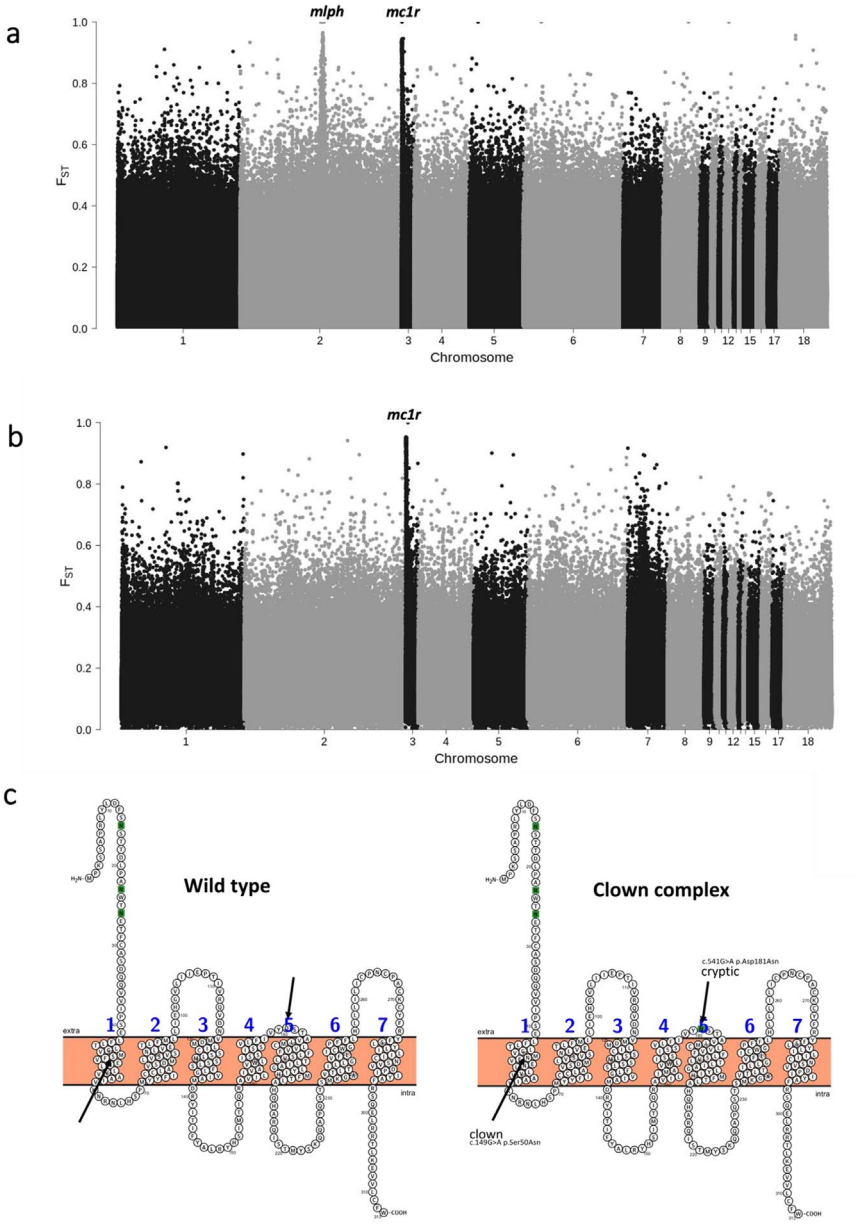

FIGURE 2 | (a) Manhattan plot (*Python_molurus_bivittatus-5.0.2_HiC* assembly) of F_{ST} values for the Clown phenotype (case) against a reference pool (control). It was established through pedigree data that control samples do not have the Clown mutation, but they all carry the mutation responsible for the Hypo–Ghost colour morph. The candidate gene for Clown maps within the peak on Chromosome 3. The peak on Chromosome 2 contains the candidate gene (*mlph*) of the Hypo–Ghost colour morph (Lederer et al. 2023). (b) Manhattan plot of F_{ST} values between Clown ($n = 38$) and Spider control pool ($n = 26$). (c) On Chromosome 3, a missense mutation (p.Ser50Asn) in the protein coding region of the *melanocortin-1 receptor* (*mc1r*) gene is associated with the Clown phenotype. The putative Clown variant is located in the first transmembrane domain of *mc1r*. The candidate Cryptic missense variant (p.Asp181Asn) maps to the extracellular region between the fourth and fifth intracellular domains. The Clown and Cryptic loci are indicated by an arrow on the wild type and Clown complex models. The green square corresponds to the N-glyco motif.

We checked the location of the SNP with the most significant changes (chromosome 3: 1,243,403), which can be seen on a zoomed-in chromosome 3 (Figure S4) and maps to an intergenic region between the uncharacterised gene LOC112541545 and *CBFA2T3* (*CBFA2*/*RUNX1* Partner Transcriptional Co-Repressor 3). These genes have not been linked to animal colouration previously. We cross-referenced SNPs with an F_{ST} greater than 0.90 (*popoolation2* output) with the annotated VCF file and found one protein-altering SNP (c.149G>A), corresponding to a missense mutation in *melanocortin-1 receptor* (*MC1R*—p.Ser50Asn). However, further inspection of the VCF file showed nine missense SNPs across seven genes—*ZFHX3, COG8*, *CDH1*, *MC1R*, *SPG7*, *PIEZO1*, *IL17C* (Table S7). These variants did not meet *popoolation2*'s filtering criteria (e.g., coverage depth, allele frequency, data completeness across populations).

Given that *MC1R* is the likely genetic basis for the Clown phenotype (genotype $MC1R^{149A}/^{149A}$), and that Clown and Cryptic are allelic, we hypothesised that a different variant on *MC1R* might

be associated with Cryptic. PCR amplification of the *MC1R* locus (3:792,150–793,091) in Cryptic, non-Cryptic, and heterozygous for Cryptic samples sent by breeders (see Section 2; Table S4) shows a distinct missense variant in *MC1R* (c.541G>A) associated with Cryptic (genotype $MC1R^{541A/541A}$), 491 bp downstream from the Clown mutation. This SNP is expected to change the amino acid sequence from aspartate to asparagine (p.Asp181Asn). A multiple sequence alignment of *MC1R* from various vertebrate species shows that the candidate Clown mutation occurs on a conserved residue, whereas the Cryptic mutation is located at a more variable site (Figure S5).

3.2 | Histological Analysis of Clown Ball Python Skin

It has recently been shown that the black skin of wild-type ball pythons contains epidermal and dermal melanophores. In the brown skin of the wild type, the number of epidermal melanophores is reduced and xanthophores are present. Iridophores are absent from the wild-type ball python skin (Tzika 2024). Here, we present histological and electron microscopy imaging data from three different skin regions of a single Clown individual (Figure 3). As for the wild type, black dorsal skin is populated by dermal and epidermal melanophores (Figure 3a,b). The number of dermal melanophores is reduced in the brown dorsal skin (Figure 3c), compared to the black dorsal skin, as has been described in other polymorphic species (Murakami, Hasegawa, and Kuriyama 2016), and the xanthophores present have xanthosomes with dense concentric lamella (Figure 3d). Only scarce epidermal melanophores are present in the yellow lateral skin and the dermal melanophores seem completely absent (Figure 3e). In this region, we find xanthophores with early stage xanthosomes that contain amorphous material instead of lamella (Figure 3f). As expected, no iridophores were found in the three skin regions of the Clown individual.

In terms of chromatophore ultrastructure, the only difference we observe compared to the wild type is the presence of melanophores with early-stage melanosomes in the dorsal black skin (inset in Figure 3b). This difference might be due to the young age of the Clown animal sampled, a one-year-old juvenile, whereas the wild-type previously studied was three-years old (Tzika 2024). Otherwise, the size and shape of the melanosomes is the same. Such differences in the maturation stage between juvenile and adult snakes have already been described for the corn snake (Ullate-Agote et al. 2020). Thus, the differences in the skin colouration pattern and pigmentation intensity observed in Clown ball pythons are probably due to the modified migration and number of melanophores, rather than changes in their ultrastructure.

4 | Discussion

In this study, we identified two distinct missense mutations in *MC1R* as putatively responsible for the Clown and Cryptic ball python colour morphs, respectively. The Agouti/MSH/MC1R signalling system (Barsh 1996) plays an important role in melanin pigmentation. In mammalian and avian systems, melanin colouration can vary from beige/yellow to black/brown. If the melanin-stimulating hormone (MSH) binds to the melanocortin receptor (MC1R), melanocytes produce black or dark brown eumelanin. However, MSH/MC1R signalling is inhibited by the binding of Agouti-signalling protein (ASIP) to MC1R, resulting in the production of pheomelanin, which imparts a yellow or reddish-brown hue. Thus, MC1R signalling is generally thought to primarily affect the hue imparted by melanin.

Mutations in *MC1R* and its antagonist, *agouti*, have been associated with adaptive phenotypes in various vertebrates, including mice and lizards (Nachman, Hoekstra, and D'Agostino 2003; Rosenblum, Hoekstra, and Nachman 2004; Nunes et al. 2011; Barrett et al. 2019; reviewed by Harris et al. 2020). Amino acid changes in transmembrane domains have been linked to melanic or red phenotypes in cattle breeds (Matsumoto et al. 2020; Hauser et al. 2022), birds (Theron et al. 2001; San-Jose et al. 2017) and reptiles (Nunes et al. 2011), although until now not in snakes (but see Cox, Rabosky, and Chippindale 2013). In humans, variations in *MC1R* are associated with the production of pheomelanin in red hair (Zorina-Lichtenwalter et al. 2019), as well as the development of cancer (Pavan and Sturm 2019; Manganelli et al. 2021). Loss-of-function mutations to *MC1R* have also been found in depigmented cavefish (Gross, Borowsky, and Tabin 2009).

The *MC1R* gene codes for a seven transmembrane G-protein-coupled receptor with intracellular and extracellular regions. Transmembrane domains help maintain the structural integrity of *MC1R* and are important for ligand-receptor interactions and melanin pigmentation (Yang et al. 1997; Rosenblum et al. 2010; Mandal et al. 2020). The Clown morph's missense mutation occurs in the first transmembrane region, while the Cryptic morph's mutation is in the extracellular loop between the fourth and fifth transmembrane domains (Figure 2c). Rosenblum, Hoekstra, and Nachman (2004) investigated the evolutionary rates of *MC1R* in mammals and squamates, showing that extracellular regions evolve the fastest, followed by transmembrane regions, with intracellular regions evolving the slowest. This suggests that intracellular and transmembrane regions are more crucial for the protein's function compared to extracellular regions. Consequently, the phenotypic variation observed in Cryptic likely results from a hypomorphic mutation (partial loss of receptor function), rather than a complete loss of function. Since the loss of function is only partial, selection pressure against mutations like D181N should be weaker compared to mutations such as S50N, as supported by the multiple sequence alignment. Therefore, it is expected that the missense mutation of the Clown morph in a transmembrane region would have greater impact on fitness than the missense mutations of the Cryptic morph in an extracellular region.

It is not unusual for different mutations on the same gene to result in different phenotypes. For example, in C57BL/6 mice the Mc1re allele turns the mouse coat to yellow (https://www.informatics.jax.org/allele/MGI:1856028) and on the same genetic background the Mc1rm1Btlr allele results in tan coloured fur (https://www.informatics.jax.org/allele/MGI:5049874). Although the *MC1R* variants discovered with this study are the likely cause of the Clown and Cryptic phenotypes in ball pythons, we did not verify if large indels or structural mutations are present in the interval. This type of analysis will be possible

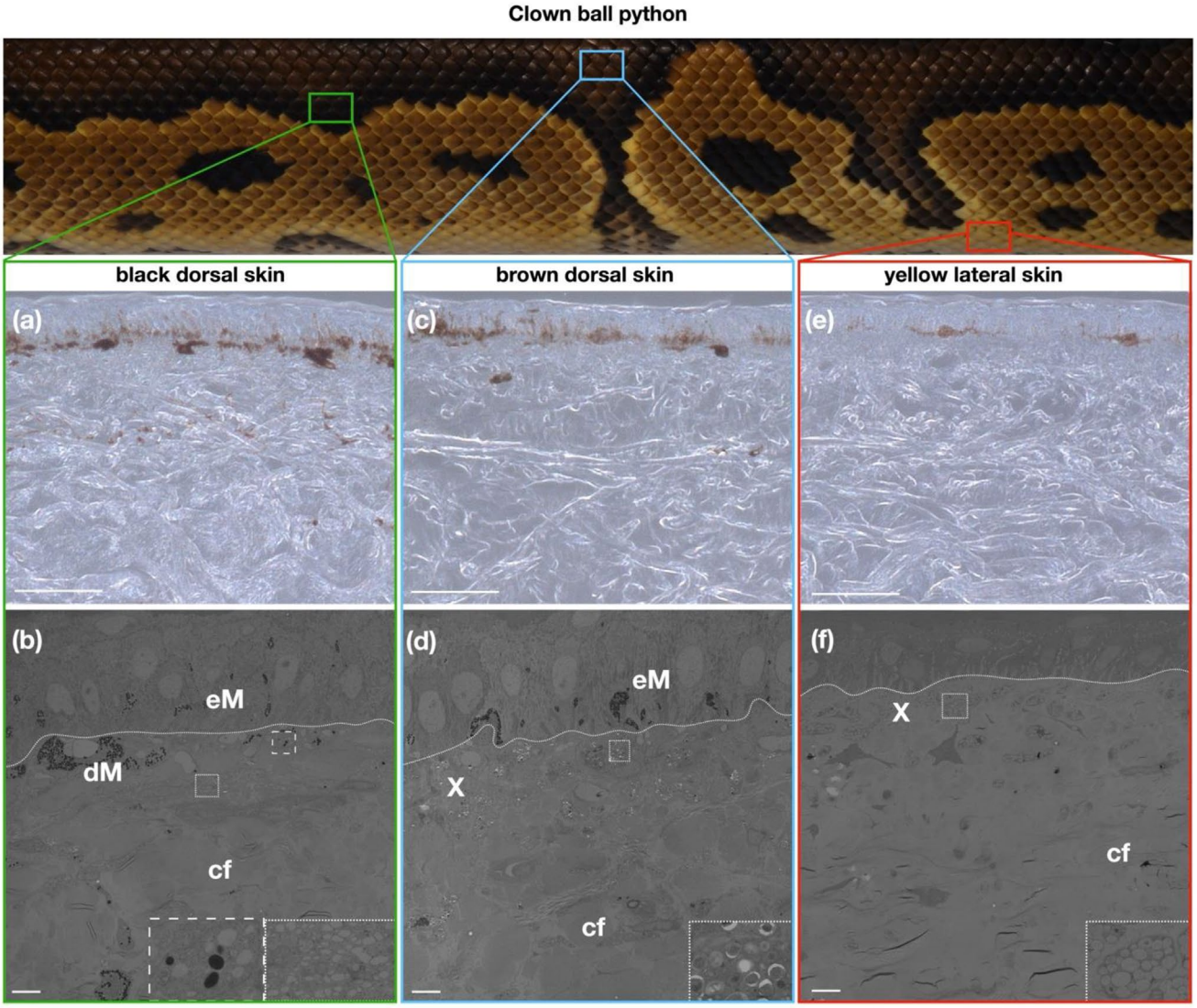

FIGURE 3 | Histological analysis of Clown ball python skin. Images of deparaffinised skin sections and transmission electron microscopy (TEM) micrographs of the black dorsal skin (a, b), the brown dorsal skin (c, d), and the yellow lateral skin (e, f). Insets in (b) focus on the early-stage melanosomes. Insets in (d) and (f) magnify the mature and the early stage xanthosomes, respectively. cf., collagen fibres; dM, dermal melanophores; eM, epidermal melanophores; X, xanthophores. Brightfield images scale bars: 50 μm, TEM scale bars: 5 μm.

when a chromosome-level assembly of the ball python genome becomes available. Additionally, functional validation, for example with CRISPR-Cas9 gene-editing, is necessary to confirm our findings.

Interactions of iridophores and xanthophores with melanophores play a role in pattern formation in zebrafish (Frohnhöfer et al. 2013; Singh, Schach, and Nüsslein-Volhard 2014; Singh and Nüsslein-Volhard 2015; Gur et al. 2020). In zebrafish, *MC1R* is involved in the countershading, that is, the absence of stripes on the ventral side of the fish (Cal et al. 2019). Indeed, an expansion of melanophores and xanthophores ventrally is observed in zebrafish *MC1R* knockouts, where normally only iridophores are found. Our study of ball python pigmentation suggests that *MC1R* might also be involved in pattern formation in reptiles. Note that a recent study of the Terrazzo corn snake morph (Tzika et al. 2024) provides evidence that the Premelanosome protein (PMEL), another important protein for melanogenesis, is also involved in the establishment of the wild type skin pattern. In combination with our findings, these results support the dual role these molecules of the melanogenesis pathway may play in colour patterning processes in snake skin colouration.

Little is known of the chromatophore interactions that establish the skin colouration patterning during development in reptiles (Ullate-Agote and Tzika 2024; Tzika et al. 2024), but we can make some inferences from the Clown phenotype and other colour morphs. In ball pythons, certain colour morphs with altered melanin pigmentation, including Clown, show an expansion of yellow colouration (Figure 1d and Figure S6). A recent study by Tzika (2024) showed that wild type ball pythons do not have iridophores, as is the case for the Clown ball pythons analysed here. Albino ball pythons, which are likely to carry melanophores that do not produce melanin similarly to amelanistic corn snakes (Saenko et al. 2015), can

be used to observe what xanthophore patterning looks like in the wild type (Figure 1c). Yellow colouration is observed in the corresponding brown regions of the wild type, and white in the regions that are normally black. Albino-Clown double mutant reveals an expanded distribution of the xanthophores (Figure 1d and Figure S6f), not only laterally, but also along the dorsal midline, where they are absent in the wild type. A similar pattern of xanthophore expansion can be observed in other Albino double mutants (e.g., Figure S6c–f). In melanic morphs (Figure S6g,h), which are characterised by an all-black phenotype, the opposite is observed. As has been documented in melanic lizards (Kuriyama et al. 2016), Albino-melanic double mutants reveal a loss of xanthophore pigmentation, or an all-white snake. Based on the co-existence of melanophores and xanthophores in this region, we can thus speculate that the *MC1R* mutation impacts the survival and/or the migration of melanophores during development, and possibly their interaction with xanthophores. Our results provide new research avenues for the study of vertebrate skin colouration and pattern formation, highlighting the utility of using captive-bred reptiles in pigmentation research. The pet trade also provides a useful system for exploring these genetic mechanisms that would be difficult to study with wild populations, where these variants are presumably kept at very low frequencies due to negative selection.

Author Contributions

A.G.-E., A.P.H., and R.D.H.B. conceived and designed the study. H.L.R. and A.C.T. collected samples. A.G.-E. and J.M.A. were responsible for the pre-sequencing molecular work (e.g., DNA extraction, quantification, and pooling). A.G.-E. performed the bioinformatics. H.L.R. was responsible for validating mutations using PCR. A.C.T. performed the histological analyses. J.W. performed molecular and genotyping analyses on European samples. A.G.-E. and A.C.T. wrote the manuscript with revisions from all authors.

Acknowledgments

This work was supported by an NSERC Discovery Grant and Canada Research Chair to R.D.H.B. and A.P.H., a Canada Research Chair to R.D.H.B., and a Swiss National Science Foundation grant (310030_204466) to A.C.T. We thank Mutation Creation, T Dot Exotics, The Ball Room Canada, and Designing Morphs for supplying samples.

Conflicts of Interest

The authors declare no conflicts of interest.

Data Availability Statement

The data that support the findings of this manuscript is available at the NCBI Sequence Read Archive (SRA), under accession PRJNA1123767.

References

Andrade, P., and M. Carneiro. 2021. "Pterin-Based Pigmentation in Animals." *Biology Letters* 17, no. 8: 20210221.

Barrett, R. D., S. Laurent, R. Mallarino, et al. 2019. "Linking a Mutation to Survival in Wild Mice." *Science* 363, no. 6426: 499–504.

Barsh, G. S. 1996. "The Genetics of Pigmentation: From Fancy Genes to Complex Traits." *Trends in Genetics* 12, no. 8: 299–305.

Baxter, L. L., L. Hou, S. K. Loftus, and W. J. Pavan. 2004. "Spotlight on Spotted Mice: A Review of White Spotting Mouse Mutants and Associated Human Pigmentation Disorders." *Pigment Cell Research* 17, no. 3: 215–224.

Baxter, L. L., D. E. Watkins-Chow, W. J. Pavan, and S. K. Loftus. 2019. "A Curated Gene List for Expanding the Horizons of Pigmentation Biology." *Pigment Cell & Melanoma Research* 32, no. 3: 348–358.

Bechtel, H. B. 1991. "Inherited Color Defects: Comparison Between Humans and Snakes." *International Journal of Dermatology* 30, no. 4: 243–246.

Brown, A. R., K. Comai, D. Mannino, et al. 2022. "A Community-Science Approach Identifies Genetic Variants Associated With Three Color Morphs in Ball Pythons (*Python regius*)." *PLoS One* 17, no. 10: e0276376.

Cal, L., P. Suarez-Bregua, I. Braasch, et al. 2019. "Loss-of-Function Mutations in the Melanocortin 1 Receptor Cause Disruption of Dorso-Ventral Countershading in Teleost Fish." *Pigment Cell & Melanoma Research* 32, no. 6: 817–828.

Caro, T. 2017. "Wallace on Coloration: Contemporary Perspective and Unresolved Insights." *Trends in Ecology & Evolution* 32, no. 1: 23–30.

Castle, W. E., and S. Wright. 1915. "Two Color Mutations of Rats Which Show Partial Coupling." *Science* 42, no. 1075: 193–195.

Castoe, T. A., A. J. De Koning, K. T. Hall, et al. 2013. "The Burmese Python Genome Reveals the Molecular Basis for Extreme Adaptation in Snakes." *Proceedings of the National Academy of Sciences* 110, no. 51: 20645–20650.

Cingolani, P., A. Platts, L. L. Wang, et al. 2012. "A Program for Annotating and Predicting the Effects of Single Nucleotide Polymorphisms, SnpEff: SNPs in the Genome of *Drosophila melanogaster* Strain w1118; Iso-2; Iso-3." *Fly* 6, no. 2: 80–92.

Côte, J., A. Boniface, S. Blanchet, A. P. Hendry, J. Gasparini, and L. Jacquin. 2018. "Melanin-Based Coloration and Host–Parasite Interactions Under Global Change." *Proceedings of the Royal Society B: Biological Sciences* 285, no. 1879: 20180285.

Cott, H. B. 1940. *Adaptive Coloration in Animals*. London, UK: Methuen & Co.

Cox, C. L., A. R. D. Rabosky, and P. T. Chippindale. 2013. "Sequence Variation in the Mc1r Gene for a Group of Polymorphic Snakes." *Gene* 513, no. 2: 282–286.

Cuthill, I. C., W. L. Allen, K. Arbuckle, et al. 2017. "The Biology of Color." *Science* 357, no. 6350: eaan0221.

Dao, U. M., I. Lederer, R. L. Tabor, B. Shahid, C. W. Graves, and H. S. Seidel. 2023. "Stripes and Loss of Color in Ball Pythons (*Python regius*) are Associated With Variants Affecting Endothelin Signaling." *G3: Genes, Genomes, Genetics* 13, no. 7: jkad063.

D'Cruze, N., S. Paterson, J. Green, et al. 2020. "Dropping the Ball? The Welfare of Ball Pythons Traded in the EU and North America." *Animals* 10, no. 3: 413.

Ducrest, A. L., L. Keller, and A. Roulin. 2008. "Pleiotropy in the Melanocortin System, Coloration and Behavioural Syndromes." *Trends in Ecology & Evolution* 23, no. 9: 502–510.

Dudchenko, O., S. S. Batra, A. D. Omer, et al. 2017. "De Novo Assembly of the *Aedes aegypti* Genome Using Hi-C Yields Chromosome-Length Scaffolds." *Science* 356, no. 6333: 92–95.

Dudchenko, O., M. S. Shamim, S. S. Batra, et al. 2018. "The Juicebox Assembly Tools Module Facilitates De Novo Assembly of Mammalian Genomes with Chromosome-Length Scaffolds for under $1000." BioRxiv, 254797. Preprint. https://doi.org/10.1101/254797.

Edgar, R. C. 2004. "MUSCLE: Multiple Sequence Alignment With High Accuracy and High Throughput." *Nucleic Acids Research* 32, no. 5: 1792–1797.

Endler, J. A., and J. Mappes. 2017. "The Current and Future State of Animal Coloration Research." *Philosophical Transactions of the Royal Society, B: Biological Sciences* 372, no. 1724: 20160352.

Frohnhöfer, H. G., J. Krauss, H. M. Maischein, and C. Nüsslein-Volhard. 2013. "Iridophores and Their Interactions With Other Chromatophores Are Required for Stripe Formation in Zebrafish." *Development* 140, no. 14: 2997–3007.

Garcia-Elfring, A., C. E. Sabin, A. L. Iouchmanov, et al. 2023. "Piebaldism and Chromatophore Development in Reptiles Are Linked to the Tfec Gene." *Current Biology* 33, no. 4: 755–763.

Gross, J. B., R. Borowsky, and C. J. Tabin. 2009. "A Novel Role for Mc1r in the Parallel Evolution of Depigmentation in Independent Populations of the Cavefish *Astyanax mexicanus*." *PLoS Genetics* 5, no. 1: e1000326.

Gur, D., E. J. Bain, K. R. Johnson, et al. 2020. "In Situ Differentiation of Iridophore Crystallotypes Underlies Zebrafish Stripe Patterning." *Nature Communications* 11, no. 1: 6391.

Harris, R. B., K. Irwin, M. R. Jones, et al. 2020. "The Population Genetics of Crypsis in Vertebrates: Recent Insights From Mice, Hares, and Lizards." *Heredity* 124, no. 1: 1–14.

Hauser, M., H. Signer-Hasler, L. Küttel, et al. 2022. "Identification of Two New Recessive MC1R Alleles in Red-Coloured Evolèner Cattle and Other Breeds." *Animal Genetics* 53, no. 3: 427–435.

Hauswirth, R., B. Haase, M. Blatter, et al. 2012. "Mutations in MITF and PAX3 Cause "Splashed White" and Other White Spotting Phenotypes in Horses." *PLoS Genetics* 8, no. 4: e1002653.

Irion, U., H. G. Frohnhöfer, J. Krauss, et al. 2014. "Gap Junctions Composed of Connexins 41.8 and 39.4 Are Essential for Colour Pattern Formation in Zebrafish." *eLife* 3: e05125.

Irizarry, K. J., and R. L. Bryden. 2016. "In Silico Analysis of Gene Expression Network Components Underlying Pigmentation Phenotypes in the Python Identified Evolutionarily Conserved Clusters of Transcription Factor Binding Sites." *Advances in Bioinformatics* 2016: 1–27.

Iwanishi, S., S. Zaitsu, H. Shibata, and E. Nitasaka. 2018. "An Albino Mutant of the Japanese Rat Snake (*Elaphe climacophora*) Carries a Nonsense Mutation in the Tyrosinase Gene." *Genes & Genetic Systems* 93, no. 4: 163–167.

Kelsh, R. N., M. Brand, Y. J. Jiang, et al. 1996. "Zebrafish Pigmentation Mutations and the Processes of Neural Crest Development." *Development* 123, no. 1: 369–389.

Kelsh, R. N., M. L. Harris, S. Colanesi, and C. A. Erickson. 2009. "Stripes and Belly-Spots—A Review of Pigment Cell Morphogenesis in Vertebrates." *Seminars in Cell & Developmental Biology* 20, no. 1: 90–104.

Kimura, T. 2021. "Pigments in Teleosts and Their Biosynthesis." In *Pigments, Pigment Cells and Pigment Patterns*, 127–148. Singapore: Springer.

Kofler, R., P. Orozco-terWengel, N. De Maio, et al. 2011. "PoPoolation: A Toolbox for Population Genetic Analysis of Next Generation Sequencing Data From Pooled Individuals." *PLoS One* 6, no. 1: e15925.

Kofler, R., R. V. Pandey, and C. Schlötterer. 2011. "PoPoolation2: Identifying Differentiation Between Populations Using Sequencing of Pooled DNA Samples (Pool-Seq)." *Bioinformatics* 27, no. 24: 3435–3436.

Kõressaar, T., M. Lepamets, L. Kaplinski, K. Raime, R. Andreson, and M. Remm. 2018. "Primer3_masker: Integrating Masking of Template Sequence With Primer Design Software." *Bioinformatics* 34, no. 11: 1937–1938.

Kõressaar, T., and M. Remm. 2007. "Enhancements and Modifications of Primer Design Program Primer3." *Bioinformatics* 23, no. 10: 1289–1291.

Kuriyama, T., K. Miyaji, M. Sugimoto, and M. Hasegawa. 2006. "Ultrastructure of the Dermal Chromatophores in a Lizard (Scincidae: Plestiodon Latiscutatus) With Conspicuous Body and Tail Coloration." *Zoological Science* 23, no. 9: 793–799.

Kuriyama, T., T. Okamoto, K. Miyaji, and M. Hasegawa. 2016. "Iridophore-and Xanthophore-Deficient Melanistic Color Variant of the Lizard Plestiodon Latiscutatus." *Herpetologica* 72, no. 3: 189–195.

Lederer, I., B. Shahid, U. Dao, et al. 2023. "A Frameshift Variant in the Melanophilin Gene Is Associated With Loss of Pigment From Shed Skin in Ball Pythons (*Python regius*)." *Micropublication Biology* 2023. https://doi.org/10.17912/micropub.biology.000896.

Li, H., and R. Durbin. 2009. "Fast and Accurate Short Read Alignment With Burrows–Wheeler Transform." *Bioinformatics* 25, no. 14: 1754–1760.

Li, H., B. Handsaker, A. Wysoker, et al. 2009. "The Sequence Alignment/Map Format and SAMtools." *Bioinformatics* 25, no. 16: 2078–2079.

Lyon, M. F. 1963. "Attempts to Test the Inactive-X Theory of Dosage Compensation in Mammals." *Genetics Research* 4, no. 1: 93–103.

Mandal, B. K., H. Chen, Z. Si, et al. 2020. "Shrunk and Scattered Black Spots Turn Out due to MC1R Knockout in a White-Black Oujiang Color Common Carp (*Cyprinus carpio* Var. Color)." *Aquaculture* 518: 734822.

Manganelli, M., S. Guida, A. Ferretta, et al. 2021. "Behind the Scene: Exploiting Mc1r in Skin Cancer Risk and Prevention." *Genes* 12, no. 7: 1093.

Matsumoto, H., M. Kojya, H. Takamuku, et al. 2020. "MC1R c. 310G>- and c. 871G>A Determine the Coat Color of Kumamoto Sub-Breed of Japanese Brown Cattle." *Animal Science Journal* 91, no. 1: e13367.

McNamara, M. E., V. Rossi, T. S. Slater, et al. 2021. "Decoding the Evolution of Melanin in Vertebrates." *Trends in Ecology & Evolution* 36: 430–443.

Megía-Palma, R., A. Jorge, and S. Reguera. 2018. "Raman Spectroscopy Reveals the Presence of Both Eumelanin and Pheomelanin in the Skin of Lacertids." *Journal of Herpetology* 52, no. 1: 67–73.

Mills, M. G., and L. B. Patterson. 2009. "Not Just Black and White: Pigment Pattern Development and Evolution in Vertebrates." *Seminars in Cell & Developmental Biology* 20, no. 1: 72–81.

Murakami, A., M. Hasegawa, and T. Kuriyama. 2016. "Pigment Cell Mechanism of Postembryonic Stripe Pattern Formation in the Japanese Four-Lined Snake." *Journal of Morphology* 277, no. 2: 196–203.

Nachman, M. W., H. E. Hoekstra, and S. L. D'Agostino. 2003. "The Genetic Basis of Adaptive Melanism in Pocket Mice." *Proceedings of the National Academy of Sciences* 100, no. 9: 5268–5273.

Nunes, V. L., A. Miraldo, M. A. Beaumont, R. K. Butlin, and O. S. Paulo. 2011. "Association of Mc1r Variants With Ecologically Relevant Phenotypes in the European Ocellated Lizard, Lacerta Lepida." *Journal of Evolutionary Biology* 24, no. 10: 2289–2298.

Olsson, M., D. Stuart-Fox, and C. Ballen. 2013. "Genetics and Evolution of Colour Patterns in Reptiles." *Seminars in Cell & Developmental Biology* 24, no. 6-7: 529–541.

Omasits, U., C. H. Ahrens, S. Müller, and B. Wollscheid. 2014. "Protter: Interactive Protein Feature Visualization and Integration With Experimental Proteomic Data." *Bioinformatics* 30, no. 6: 884–886.

Patterson, L. B., and D. M. Parichy. 2019. "Zebrafish Pigment Pattern Formation: Insights Into the Development and Evolution of Adult Form." *Annual Review of Genetics* 53: 505–530.

Pavan, W. J., and R. A. Sturm. 2019. "The Genetics of Human Skin and Hair Pigmentation." *Annual Review of Genomics and Human Genetics* 20: 41–72.

Rosenblum, E. B., H. E. Hoekstra, and M. W. Nachman. 2004. "Adaptive Reptile Color Variation and the Evolution of the MCIR Gene." *Evolution* 58, no. 8: 1794–1808.

Rosenblum, E. B., H. Römpler, T. Schöneberg, and H. E. Hoekstra. 2010. "Molecular and Functional Basis of Phenotypic Convergence in

White Lizards at White Sands." *Proceedings of the National Academy of Sciences* 107, no. 5: 2113–2117.

Saenko, S. V., S. Lamichhaney, A. Martinez Barrio, N. Rafati, L. Andersson, and M. C. Milinkovitch. 2015. "Amelanism in the Corn Snake Is Associated With the Insertion of an LTR-Retrotransposon in the OCA2 Gene." *Scientific Reports* 5: 17118.

Saenko, S. V., J. Teyssier, D. van der Marel, and M. C. Milinkovitch. 2013. "Precise Colocalization of Interacting Structural and Pigmentary Elements Generates Extensive Color Pattern Variation in Phelsumalizards." *BMC Biology* 11, no. 1: 1–13.

San-Jose, L. M., A. L. Ducrest, V. Ducret, et al. 2017. "MC 1R Variants Affect the Expression of Melanocortin and Melanogenic Genes and the Association Between Melanocortin Genes and Coloration." *Molecular Ecology* 26, no. 1: 259–276.

Shumate, A., and S. L. Salzberg. 2021. "Liftoff: Accurate Mapping of Gene Annotations." *Bioinformatics* 37, no. 12: 1639–1643.

Singh, A. P., and C. Nüsslein-Volhard. 2015. "Zebrafish Stripes as a Model for Vertebrate Colour Pattern Formation." *Current Biology* 25, no. 2: R81–R92.

Singh, A. P., U. Schach, and C. Nüsslein-Volhard. 2014. "Proliferation, Dispersal and Patterned Aggregation of Iridophores in the Skin Prefigure Striped Colouration of Zebrafish." *Nature Cell Biology* 16, no. 6: 604–611.

Starck, J. M., F. Schrenk, S. Schröder, and M. Pees. 2022. "Malformations of the Sacculus and the Semicircular Canals in Spider Morph Pythons." *PLoS One* 17, no. 8: e0262788.

Subkhankulova, T., K. Camargo Sosa, L. A. Uroshlev, et al. 2023. "Zebrafish Pigment Cells Develop Directly From Persistent Highly Multipotent Progenitors." *Nature Communications* 14, no. 1: 1258.

Theron, E., K. Hawkins, E. Bermingham, R. E. Ricklefs, and N. I. Mundy. 2001. "The Molecular Basis of an Avian Plumage Polymorphism in the Wild: A Melanocortin-1-Receptor Point Mutation is Perfectly Associated With the Melanic Plumage Morph of the Bananaquit, *Coereba flaveola*." *Current Biology* 11, no. 8: 550–557.

Toomey, M. B., C. I. Marques, P. M. Araújo, et al. 2022. "A Mechanism for Red Coloration in Vertebrates." *Current Biology* 32, no. 19: 4201–4214.

Tzika, A. C. 2024. "On the Role of TFEC in Reptilian Coloration." *Frontiers in Cell and Developmental Biology* 12: 1358828.

Tzika, A. C., A. Ullate-Agote, P. Y. Helleboid, and M. Kummrow. 2024. "PMEL Is Involved in Snake Colour Pattern Transition From Blotches to Stripes." *Nature Communications* 15, no. 1: 7655.

Tzika, A. C., A. Ullate-Agote, S. Zakany, M. Kummrow, and M. C. Milinkovitch. 2023. "Somitic Positional Information Guides Self-Organised Patterning of Snake Scales." *Science Advances* 9: eadf8834.

Ullate-Agote, A., I. Burgelin, A. Debry, et al. 2020. "Genome Mapping of a LYST Mutation in Corn Snakes Indicates That Vertebrate Chromatophore Vesicles Are Lysosome-Related Organelles." *Proceedings of the National Academy of Sciences* 117, no. 42: 26307–26317.

Ullate-Agote, A., and A. C. Tzika. 2024. "The Dynamic Behavior of Chromatophores Marks the Transition From Bands to Spots in Leopard Geckos." *Proceedings of the National Academy of Sciences* 121, no. 29: e2400486121.

Usui, Y., and M. Watanabe. 2021. "Role of the Connexin C-Terminus in Skin Pattern Formation of Zebrafish." *BBA Advances* 1: 100006.

Wakamatsu, K., and S. Ito. 2021. "Melanins in Vertebrates." In *Pigments, Pigment Cells and Pigment Patterns*, 45–89. Singapore: Springer Nature.

Wallace, A. R. 1882. "Dr. Fritz Müller on Some Difficult Cases of Mimicry." *Nature* 26, no. 656: 86–87.

Watanabe, M., R. Sawada, T. Aramaki, I. M. Skerrett, and S. Kondo. 2016. "The Physiological Characterization of connexin41. 8 and connexin39. 4, Which Are Involved in the Striped Pattern Formation of Zebrafish." *Journal of Biological Chemistry* 291, no. 3: 1053–1063.

Waterhouse, A. M., J. B. Procter, D. M. Martin, M. Clamp, and G. J. Barton. 2009. "Jalview Version 2—A Multiple Sequence Alignment Editor and Analysis Workbench." *Bioinformatics* 25, no. 9: 1189–1191.

Wiens, J. J., and Z. Emberts. 2024. "How Life Became Colourful: Colour Vision, Aposematism, Sexual Selection, Flowers, and Fruits." *Biological Reviews*. https://doi.org/10.1111/brv.13141.

Yang, Y. K., C. Dickinson, C. Haskell-Luevano, and I. Gantz. 1997. "Molecular Basis for the Interaction of [Nle4, d-Phe7] Melanocyte Stimulating Hormone With the Human Melanocortin-1 Receptor (Melanocyte α-MSH Receptor)." *Journal of Biological Chemistry* 272, no. 37: 23000–23010.

Zorina-Lichtenwalter, K., R. N. Lichtenwalter, D. V. Zaykin, et al. 2019. "A Study in Scarlet: MC1R as the Main Predictor of Red Hair and Exemplar of the Flip-Flop Effect." *Human Molecular Genetics* 28, no. 12: 2093–2106.

Supporting Information

Additional supporting information can be found online in the Supporting Information section.